Diseases of the Temporal Bone

Jan W. Casselman and Timothy John Beale

Imaging of the Temporal Bone Anatomy

High-resolution CT is best suited to look at the external and middle ear but can also provide information about 'the inner ear'. For many years multi-detector CT (MDCT) was the method of choice [1, 2], but recently high-end cone beam CT (CBCT) started to challenge MDCT. CBCT not only provides similar information at a substantially lower dose but high-end CBCTs are also able to produce images with a spatial resolution down to 125 μm. Subtle bone structures like the footplate, crura of the stapes, walls of the tympanic segment of the facial nerve canal, tegmen tympani, etc. can be visualised in a more reliable way at this resolution and open possibilities to more accurately depict pathology associated with these structures. An additional advantage is that images can be displayed in any plane without quality loss which is not the case on reformatted MDCT images. Therefore the difference between MDCT and CBCT even becomes more obvious on coronal or double-oblique images.

The inner ear is best studied on T2-weighted gradient-echo (CISS) or turbo spin-echo driven equilibrium (DRIVE), three dimensional turbo spin-echo (3D TSE), fast imaging employing steady state acquisition (FIESTA) MR images. The intralabyrinthine fluid can be seen as high signal intensity on these images, and the bony (modiolus and bony septa) and membranous (soft-tissue structures or membranes) have a low signal intensity on these images making it possible to distinguish, for instance, the scala tympani and scala vestibuli. For the same reasons, the facial nerve and the three-end branches of the cochleovestibular nerve can be distinguished in the fundus of the internal auditory canal (IAC) [3]. Even smaller structures like the macula utriculi, the ganglion of Scarpa and the posterior ampullar nerve can be visualised when the spatial resolution is high enough (0.3 × 0.3 × 0.7 mm, with the overlapping slices of 0.7 mm made every 0.35 mm) (Fig. 1).

The cause of deafness can also be located along the auditory pathway, and this can only be depicted on MR images. MR is able to visualise lesion at the level of the cochlear nuclei, trapezoid body, lateral lemniscus, inferior colliculus, medial geniculate body and auditory cortex [4]. The myelinated structures of the auditory and vestibular pathway can be seen as low signal intensity structures on multi-echo sequences like m-FFE, MEDIC and MERGE.

Choice Between CT and MR Depends on Clinical Presentation

CT is the preferred technique in patients with conductive hearing loss (CHL), and MR is the modality of choice in case of sensorineural hearing loss (SNHL), vertigo or tinnitus. However, both techniques can often contribute as is the case in trauma of the inner ear or cholesteatoma of the middle ear.

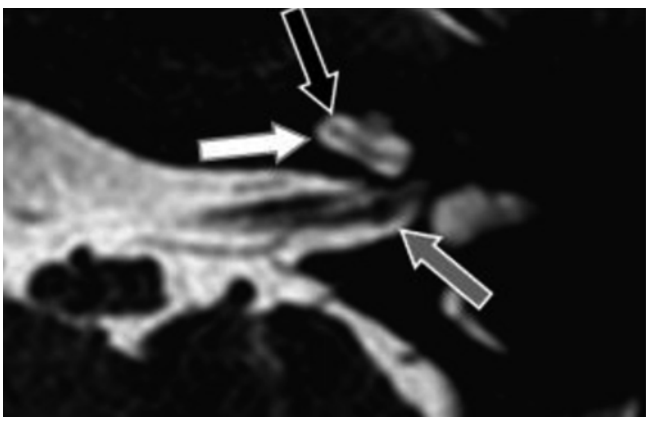

Fig. 1 3.0 T 0.7 mm thick DRIVE image with an in-plane resolution of 0.3×0.3 mm showing ganglion of Scarpa located on the superior vestibular branch of the VIIIth nerve (*grey arrow*). The separation in scala vestibuli (*black arrow*) and tympani (*white arrow*) inside the cochlea can also be seen

J.W. Casselman, MD, PhD (✉)
Radiology and Medical Imaging, AZ St-Jan Brugge-Oostende AV, Campus Bruges, Bruges, Belgium
e-mail: jan.casselman@azsintjan.be

T.J. Beale
Imaging Department, University College London, London, UK
e-mail: tim.beale@uclh.nhs.uk

J. Hodler et al. (eds.), *Diseases of the Brain, Head and Neck, Spine 2016–2019: Diagnostic Imaging*, DOI 10.1007/978-3-319-30081-8_17

In the paragraphs below, the value of CT and MR in the diagnosis of the most frequent diseases of the temporal bone will be discussed.

Pathology

Congenital External and Middle Ear Malformations

The embryology of the middle and external ear is linked, and this explains why external and middle ear malformations often occur together. In case of external auditory canal 'fibrous' or 'osseous' atresia, the middle ear cannot be evaluated by the ear surgeons, and in these cases they even totally depend on the imaging findings. In case of congenital CHL, it is crucial for the surgeons to know which ossicles or parts of the ossicles are present and available for the reconstruction of a functioning ossicular chain and whether the round and oval windows are open [5, 6]. Subtle malformations of the stapes, footplate and oval window can be the cause of congenital CHL and are today visualised in a more reliable way on high-resolution 125 μm cone beam CT images (Fig. 2). The course of the facial nerve will often shift anteriorly in the presence of external and middle ear malformations. Therefore one of the major tasks of the radiologist is to warn the surgeon for an abnormal course of the facial nerve which can be running through the middle, can split in two or more branches at the level of the mastoid segment of the nerve, etc. An abnormal course of the facial nerve and also a dehiscence of the facial nerve canal can be better visualised since high-resolution 125 μm CBCT is available.

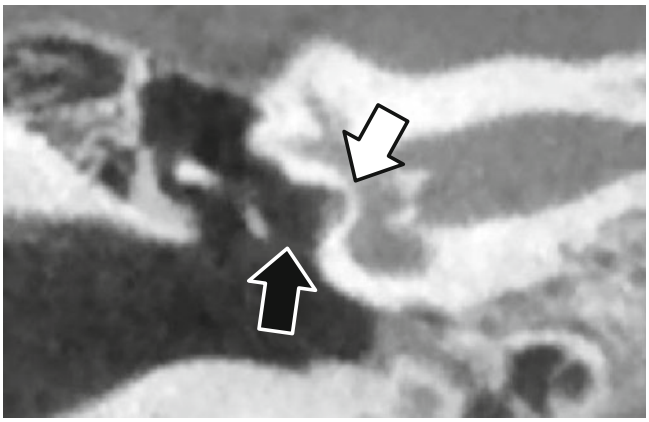

Fig. 2 Congenital conductive hearing loss caused by absent stapes (*black arrow*) and a thickened oval window or footplate (*white arrow*). Notice that the facial nerve is lying over the closed oval window and descended from its normal position under the lateral semicircular canal

Trauma

Longitudinal fractures along the long axis and transverse fractures perpendicular on the long axis of the temporal bone are best depicted on CT images with bone window settings. Longitudinal fractures most often run through the middle ear where they can cause fractures or luxation of the ossicles (Fig. 3a) and resulting CHL and they often end at the level of the geniculate ganglion where they can be at the origin of facial nerve palsy. Although CT remains the initial imaging technique in trauma of the temporal bone, [7] MR must be considered when the post-traumatic SNHL remains unexplained on CT.

Post-traumatic intralabyrinthine haemorrhage or inner ear concussion is best seen on unenhanced T1-weighted images (Fig. 3b) (DRIVE, CISS, 3D TSE, FIESTA). The high signal intensity of the fluid will disappear in case of fibrosis or cloth formation, and this is best seen on heavily T2-weighted images of the inner ear like CISS, 3D TSE, DRIVE, FIESTA, etc. However when the fluid is mixed with fresh blood, it can retain its normal high signal intensity for some time.

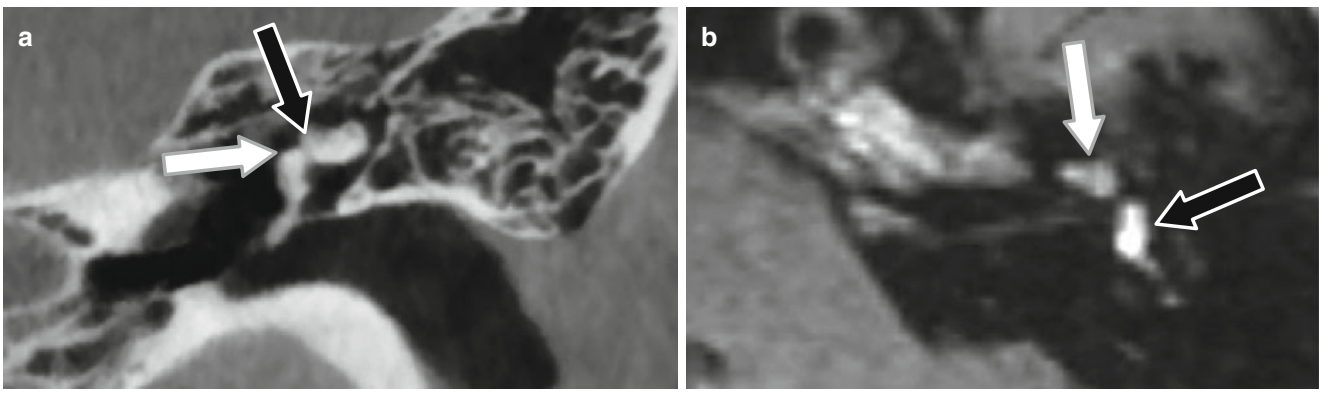

Fig. 3 (**a**) Cone beam CT. Coronal image showing an incudo-mallear luxation malleus (*white arrow*), incus (*black arrow*). (**b**): Axial unenhanced T1-weighted image showing high signal intensity blood in the labyrinth: labyrinthine concussion cochlea (*white arrow*), vestibule (*black arrow*)

Meningoceles or encephaloceles can be the result of tegmen fractures and can be distinguished from middle ear blood or inflammation on MR images [8].

Trauma to the brainstem and auditory pathways and cortex can also be the cause of SNHL or deafness. In case of haemorrhagic concussion the most frequently involved structures of the auditory pathways are the inferior colliculi and the auditory cortex. CT sometimes remains normal in patients with post-traumatic facial nerve palsy. In these patients the labyrinthine segment of the facial nerve should be checked. The labyrinthine segment occupies 95 % of the available space of the canal. Therefore post-traumatic concussion and resulting retrograde oedema can easily cause ischaemia and secondary necrosis of the labyrinthine segment itself as there is no remaining space for swelling. This can be seen as enhancement of the labyrinthine segment and enhancement near the fundus of the internal auditory canal, which is always abnormal [9]. In such a case, decompression of the nerve should be considered in order to save the facial nerve function.

Otosclerosis

The dense ivory-like endochondral bone layer around the labyrinthine capsule is replaced by foci of spongy vascular irregular new bone and causes mixed hearing loss in otosclerosis patients. Otosclerosis/otospongiosis can be fenestral and retrofenestral.

Fenestral otosclerosis is in the first place causing CHL, and hypodensities or even hypodense masses can be found on the promontory, near the facial nerve canal and close to the oval and round window. The fissula ante fenestram, just anterior to the footplate, is most frequently involved. At the level of the oval window, the footplate can be thickened, or the anterior crus of the stapes can be fixed or overgrown by otospongiosis so that the stapes can no longer move freely. This can explain the CHL in these patients. Subtle otospongiosis lesions near the footplate cannot be visualised in a strict axial or coronal plane as the footplate is angled in space. Only high-resolution double-oblique reformatted images can visualise both branches of the stapes and the footplate in one plane (Fig. 4). These double-oblique images can only be acquired when 0.1-mm thick reformatted MDCT or high-resolution 0.125 mm CBCT images are used. Successful surgery in otosclerosis is only possible when the round window is still (partially) open, and therefore these structures should always be checked preoperatively.

Retrofenestral otosclerosis is predominantly responsible for the SNHL component of the mixed hearing loss and involves the bone around the membranous labyrinth, most frequently around the cochlea. In severe case a hypodense ring can develop around the complete cochlea, but retrofenestral otosclerosis can also be limited to a small hypodense spur anterior to the antero-inferior wall of the fundus of the internal auditory canal [10, 11].

Chronic Middle Ear Inflammation

Retraction and thickening of the drum and disturbed middle ear aeration are the hallmarks of chronic middle ear inflammation. Other signs are mucosal thickening, replacement of the middle ear aeration by fluid and/or glue-like thickened material, demineralisation of the ossicles, luxation of the ossicles by inflammatory tractions, etc. However, clear destruction or displacement of the ossicles is not seen. The middle ear inflammation often follows pre-existing structures like the plicae and ligaments which form the tympanic diaphragm. This explains why the inflammation will stop at these structures and is visible as a straight barrier with the aerated part of the rest of the middle ear, a sign confirming that one is dealing with inflammation and not cholesteatoma. In completely non-aerated middle ears and mastoids, the differential diagnosis becomes more tricky as a small

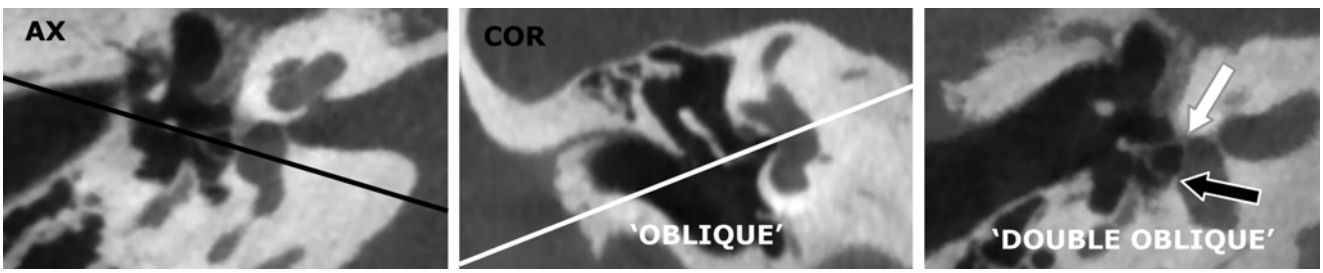

Fig. 4 The only reliable way to evaluate fenestral otosclerosis is the double-oblique technique. Para-coronal images are made on the axial image through the incudostapedial joint and perpendicular on the footplate (*black line*). Then double-oblique images are produced when reconstructions are made parallel to the incudostapedial junction on the para-coronal '*oblique*' images (*white line*). The resulting *double-oblique* images show the subtle otospongiosis at the fissula ante fenestram (*white arrow*), fixing the anterior branch of the stapes and the posterior otosclerotic footplate plaque (*black arrow*), narrowing the footplate opening

cholesteatoma can be hidden somewhere in the inflammation. In order to exclude a cholesteatoma, one should exclude displacement or erosion/destruction of the ossicles and erosion or destruction of the bony septa and/or middle ear, antrum and mastoid walls.

Finally one is dealing with tympanosclerosis (Fig. 5) when the thickened drum or inflammatory tissue in the middle ear is calcified. It is clear that CT is the imaging technique of choice to depict these middle ear changes in a reliable way.

Cholesteatoma

Cholesteatoma develops when ectoderm tissue gets trapped in the middle or inner ear (during embryology or later in life) and consists of a sac lined by keratinising stratified squamous epithelium. The diagnosis of a cholesteatoma is made when a convex soft-tissue mass is seen in the middle ear; when the ossicles are displaced, eroded and destroyed; when tympanic wall structures like the lateral wall and tegmen are eroded and destroyed; and when the scutum is amputated. The soft-tissue lesion itself will only be visible when it is surrounded by normal middle ear aeration. There is suspicion for a cholesteatoma when only one side of the lesion is convex, and the probability of a cholesteatoma becomes very high when it is completely convex. However it becomes often impossible to distinguish post-surgery changes, inflammation (recurrent), cholesteatoma, etc. when the middle ear and mastoid are completely non-aerated. This even becomes more difficult in a postoperative ear where landmarks as the integrity of the ossicles and walls of the middle ear cavity can no longer be used.

This explains why MR is today replacing CT in the diagnosis and follow-up of cholesteatoma patients. Cholesteatoma has specific signal intensities on MR: high signal intensity on T2, low signal intensity on unenhanced T1, low signal intensity on Gd-enhanced T1 but with a thin rim of enhancement around the lesion and a very high signal intensity on non-echoplanar diffusion-weighted MR images (b = 1000). Even in a completely non-aerated middle ear, the diagnosis can now be made on MR. The very high signal on echo-planar imaging diffusion-weighted imaging (non-EPI DWI) images is most specific and even allows differentiation with cholesterol granuloma and inflammation which both have a low signal intensity on non-EPI DWI. Calculated ADC maps should always be used to confirm the diagnosis as only cholesteatoma has a low signal on ADC images. It goes without saying that this technique is even more valuable in the postoperative ear and has provided us for the first time with a reliable imaging technique to rule out recurrent or residual cholesteatoma. The result is that expensive, time-consuming and for the patient unpleasant routine second-look surgery could be abolished. Partial volume still poses a problem as it is difficult to acquire diffusion-weighted MR images with a slice thickness below 2–3 mm. As a consequence very small recurrences can still be overlooked. On the other hand, there are no false positives on the non-EPI DWI MR images, which means that when a high signal is present on the b-1000 images, a cholesteatoma will be found (Fig. 6). The remaining role of CT and especially low-dose CBCT is now to provide the surgeon with a preoperative road map once a cholesteatoma or residual/recurrent cholesteatoma is found on MR [12–14].

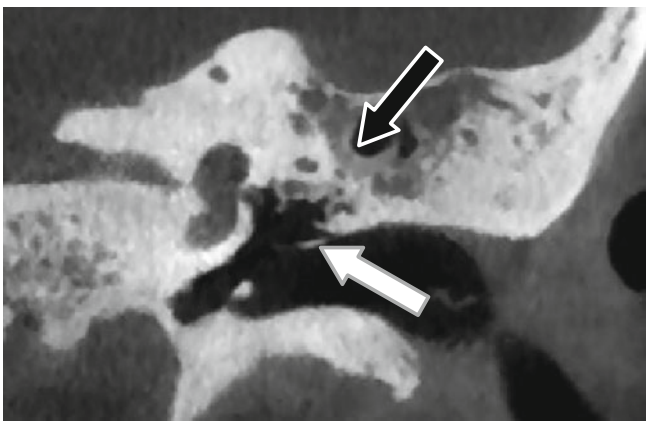

Fig. 5 Coronal cone beam CT image. Tympanosclerosis with perforation and calcification of the drum (*white arrow*) and calcifications in non-aerated part of the antrum (*black arrow*)

Cochleovestibular Schwannoma

Cochleovestibular schwannomas (CVS) are the most frequent tumours found inside the IAC and cerebellopontine angle, and the most frequent symptoms at presentation are SNHL, vertigo and tinnitus [15]. Gd-enhanced T1-weighted images are the most sensitive images to detect them. Although many of these schwannomas can also be seen on submillimetric T2-weighted images, gadolinium (Gd) administration is still needed as a schwannoma cannot be distinguished from a normal ganglion of Scarpa on these T2-weighted images, and many CVS start in the ganglion of Scarpa [16].

Once a CVS is found, the most important task of the radiologist is to exclude contralateral pathology. The detection of a contralateral schwannoma or other important middle and inner ear pathology will make the surgeon much more reluctant to remove the initially detected schwannoma. Removal of the initial schwannoma can result in a deaf ear, a risk the surgeon will not likely take when he is aware that the presence of a contralateral schwannoma or even intralabyrinthine schwannoma [17] or other middle/inner ear pathology can eventually result in bilateral deafness. In these patients the

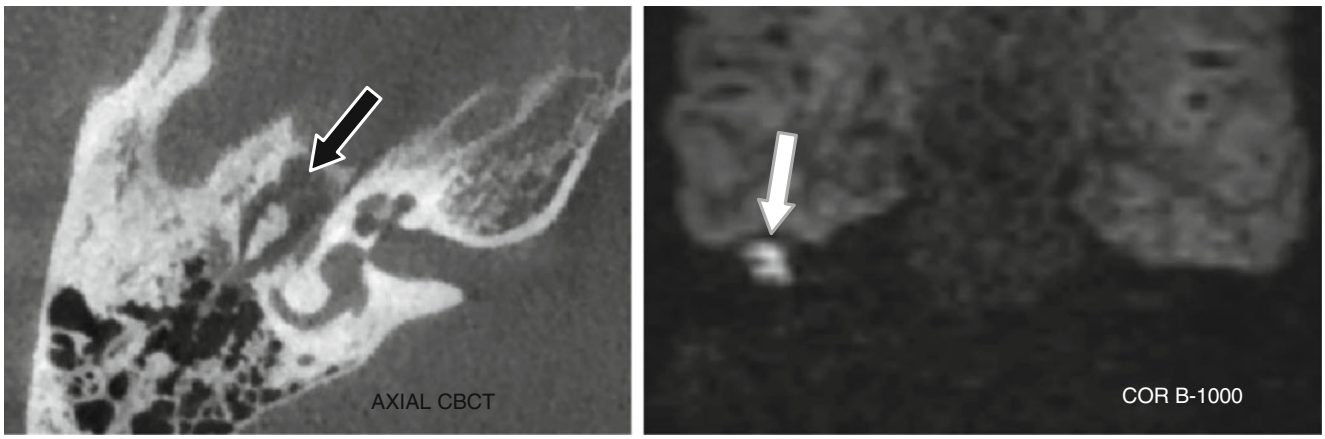

Fig. 6 *Axial CBCT* showing a completely non-aerated middle ear; a cholesteatoma cannot be ruled out. A cholesteatoma can be seen on the *B-1000* non-EPI DWI image (*white arrow*) and corresponded with the non-aerated region in the pro-epitympanum on CBCT (*black arrow*)

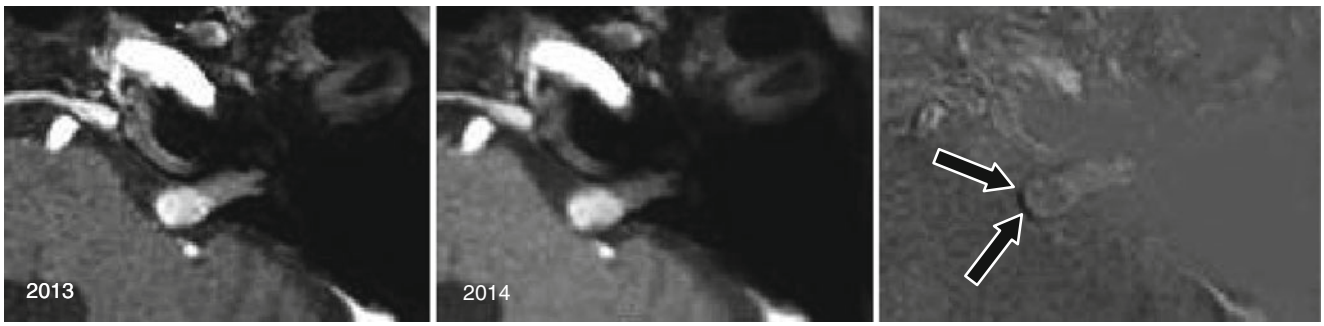

Fig. 7 Gadolinium-enhanced axial 0.6-mm thick GE T2-weighted image made in *2013* and *2014* shows a schwannoma on the left side. Volume measurements showed no growth; however subtle growth towards the cerebellopontine angle could be seen as a black rim on the subtraction images (*black arrows*)

surgeon will prefer to "follow-up and scan" until there is an important reason to remove one of the lesions.

The most important reason to remove a CVS is when it grows, and therefore its 'growth potential' must be assessed. High-resolution submillimetric T1-weighted gradient-echo images (e.g. 3DFT-MPRAGE) are best suited and can be used for volume measurements. In the first year, the follow-up studies should be acquired every 6 months and subsequently annually in case the schwannoma is not growing fast. Image subtraction is today the most sensitive technique to detect CVS growth (Fig. 7).

Submillimetric T2-weighted images are also best suited to predict whether hearing preservation surgery will be successful or not. The absence of fluid between the schwannoma and the base of the cochlea and the decrease of the signal intensity of the intralabyrinthine fluid are two bad indicators for hearing preservation [18, 19]. Hence, in such a case, the less invasive translabyrinthine approach is chosen. However, when MR indicates that hearing preservation is possible, then the surgeon will go for a suboccipital or middle cranial fossa approach.

Labyrinthitis

The calcifications in end-stage ossifying labyrinthitis are only visible on CT, while the intralabyrinthine enhancement in acute labyrinthitis (Gd enhancement) and fibrosis formation in subacute labyrinthitis are only detectable on MR (Fig. 8). In the latter case, it is not possible to distinguish fibrosis from calcifications on T2-weighted TSE or GE images. Therefore both MR and CT should be used to study patients with labyrinthitis.

Gd enhancement can be seen in viral labyrinthitis, and fibrosis formation or calcification only rarely occurs in these patients. On the contrary, fibrosis can develop quickly, and calcification can already appear in 3–4-week time in patients with bacterial meningitis (e.g. pneumococcus or meningococcus). Meningitis is more frequent in children and can result in complete deafness when both ears are affected. Urgent MR and CT imaging is needed in these children so that the surgeon has an idea about the cochlear fibrosis and/or calcification. Depending on the imaging results, the surgeon will be able to decide whether a cochlear implant can

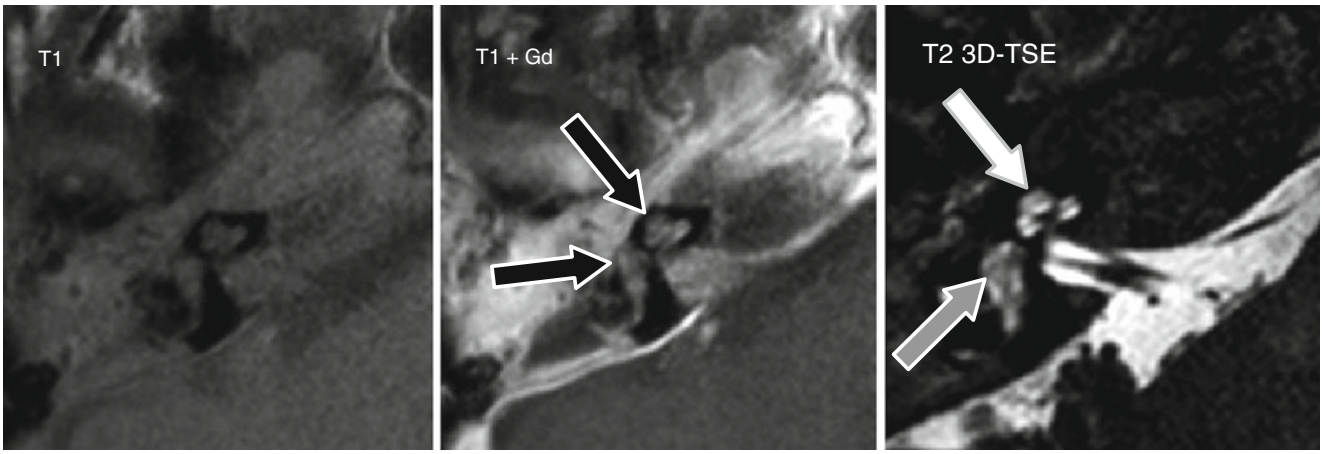

Fig. 8 Middle ear infection with secondary labyrinthitis. Low signal intensity is seen in the labyrinth on the unenhanced image. Clear enhancement is seen in the cochlea and labyrinth after intravenous Gd administration, confirming the presence of acute labyrinthitis (*black arrows*). The *T2* image shows normal fluid in the cochlea (*white arrow*), while the signal in the vestibule decreased, confirming vestibular fibrosis formation (*grey arrow*)

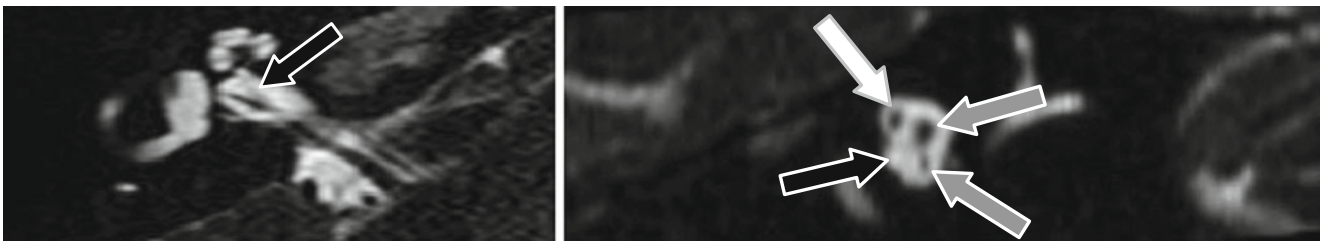

Fig. 9 Axial- and parasagittal-reformatted image through the fundus of the right internal auditory canal. The cochlear branch is absent (*black arrows*) and there is no connection with the otherwise normal cochlea. Notice the normal facial nerve (*white arrow*) and superior and inferior vestibular branches (*grey arrows*) on the parasagittal image

be installed or not and this before complete calcification sets in and makes cochlear implantation impossible. Anaesthesia is needed to examine young children, and to avoid the risks of a second anaesthesia, it is wise to perform CT and MR during the same initial imaging session [11, 20, 21].

Congenital Inner Ear Malformations

Congenital malformations of the inner ear are best studied on MR although the bony malformations can also be seen on CT. Subtle changes inside the cochlea like the absence or incomplete development of the inter- or intrascalar separations and the presence of normal fluid inside the cochlea can only be evaluated on MR. These patients present with congenital SNHL or deafness and are today best classified by using the Sennaroglu classification. A large vestibular aqueduct (CT) or enlarged endolymphatic duct and sac (MR) is the most frequent inner ear malformation. The diagnosis should not be overlooked as repetitive trauma in these patients can result in complete deafness. The second most frequent malformation is a saccular lateral semicircular canal or duct, and this malformation is most often an incidental finding without any clinical consequence. The danger of a gusher ear is always present in patients with congenital inner ear malformations. In a gusher ear, the CSF pressure is transmitted to the perilymph by defects at the base of the cochlea or fundus of the IAC. Demonstration of such a defect, a large vestibular aqueduct or an abnormal convex shape of the angle between the labyrinthine and tympanic segment of the facial nerve should warn the surgeon; however sometimes the inner ear can look completely normal on MR and CT. Surgery in such a patient will almost always result in a deaf ear and should be avoided. Finally the facial nerve can have an abnormal cause in case of inner ear malformations, and the radiologist should warn the surgeon when this is the case [5, 11, 22]! MR is also needed to demonstrate the presence of a cochleovestibular nerve or cochlear branch of the VIIIth nerve in congenital deaf cochlear implant candidates. Cochlear implantation is not possible in the absence of the VIIIth nerve or its cochlear branch (Fig. 9), and unnecessary expensive surgery and implantation can be avoided in these patients [23].

Menière's Disease: Labyrinthine Hydrops

One of the fastest growing new indications is the demonstration of endolymphatic hydrops, which is also causing the SNHL, vertigo and tinnitus in Menière's patients. The confirmation of the hydrops makes the clinicians more certain of the diagnosis, a diagnosis which is not always certain and must be confirmed when more aggressive treatment is considered. Today the hydrops can be demonstrated in a non-invasive way by using high-resolution 3D-FLAIR images made 4 h after intravenous gadolinium injection [24]. The gadolinium only has access to the perilymphatic space, and hence the scala media will remain black. This non-enhancing (black) endolymphatic utricle/saccule and scala media will enlarge in case of hydrops and will push away the surrounding enhancing perilymph in the vestibule and the enhancing perilymph in the scala vestibuli (Fig. 10).

Pathology Involving the Central Auditory Pathways

The cause of SNHL can be located along the auditory pathway, and therefore an MR study of the brainstem and auditory cortex should be performed when selective CT and MR studies of the temporal bone remain normal. Infarctions (older patients), multiple sclerosis (younger patients), trauma, tumour and inflammation located at the level of the cochlear nuclei, the trapezoid body, the lateral lemniscus, the inferior colliculus, the medial geniculate body and the auditory cortex can all cause SNHL. The SNHL will be unilateral up to the level of the cochlear nuclei and bilateral up to the level of the medial geniculate bodies, and auditory agnosia will occur when the auditory cortex gets involved. Congenital cortical pachygyria or polymicrogyria can also affect the auditory cortex and should be excluded in all cochlear implant candidates [4, 25, 26].

Tinnitus

Today patients with tinnitus can be examined in a non-invasive way using MR, with the highest sensitivity in patients with 'pulsatile' and 'objective' tinnitus. The yield is much lower in subjective and non-pulsatile tinnitus. Neurovascular conflicts near the root entry zone of the VIIIth nerve can best be recognised on gradient-echo or turbo spin-echo T2-weighted images (showing the nerves), unenhanced MRA TOF images (showing the arteries) and selective contrast-enhanced T1-weighted images (showing veins and arteries) of the temporal bone. Matching of the three sequences allows to distinguish nerves, arteries and veins in all cases. Nevertheless a neurovascular conflict is not frequently the cause of pulsatile tinnitus, and this diagnosis is often questioned. Far more frequent causes of tinnitus are paragangliomas, dural arteriovenous fistulas, idiopathic venous tinnitus and benign intracranial hypertension. Only the first two can be shown on MR.

Early venous drainage (high flow in veins) can be seen on the non-enhanced MRA TOF images in case of dural fistulas. Unenhanced and Gd-enhanced MRA TOF images are also suited to detect glomus tumours, arteriovenous malformations, aberrant vessels running through the middle ear, high or dehiscent jugular bulbs, tortuous carotid arteries near the skull base, fibromuscular dysplasia, carotid dissection, etc. Vascularised tumours like meningiomas cause a higher arte-

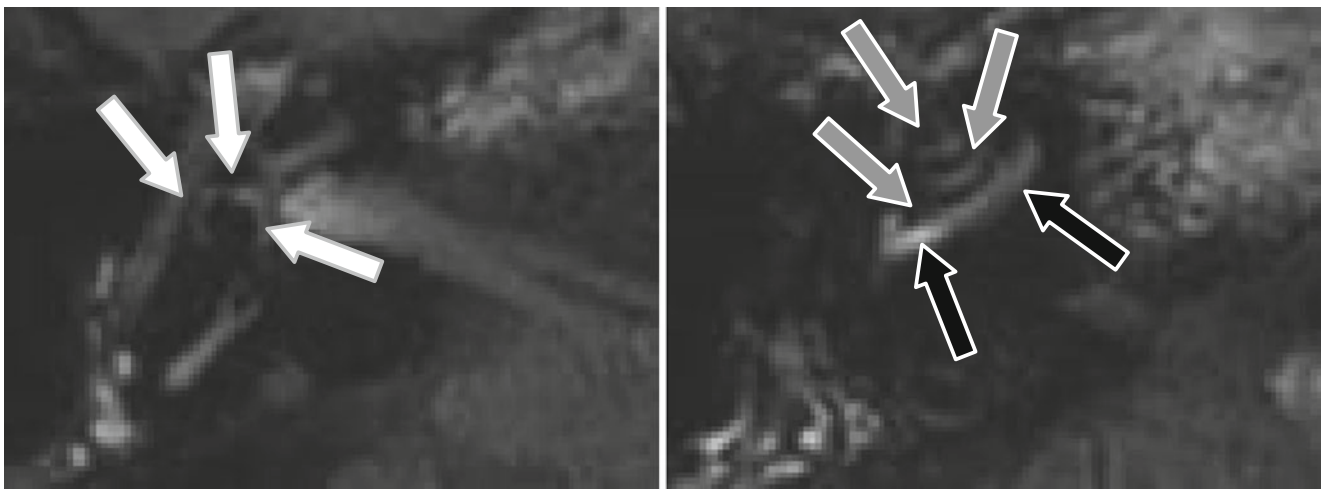

Fig. 10 Axial 3D-FLAIR images 4 h after intravenous gadolinium injection. The enlarged black saccule and utricle are confluent and compress the enhancing perilymph (*white arrows*) against the walls of the bony vestibule. The perilymph in the scala vestibuli is completely compressed by the black enlarged scala media (*grey arrows*). Normal enhancing perilymph in the scala tympani (*black arrows*) which cannot be compressed by the scala media as a bony lamina separates them

rial and venous flow in their surroundings and therefore can cause tinnitus. Hence tumours in the neighbourhood of the temporal bone must be excluded in tinnitus patients. MRA clearly became the method of first choice and detects much more causes of tinnitus than CT. However in rare cases, like Paget's disease, CT can still have its value when MRA remains negative. Today the place of angiography is limited to the treatment of tinnitus (embolisation); it will only be used for diagnostic purposes when MR and CT remain negative and the pulsatile tinnitus renders a normal life impossible [27–29].

Bibliography

1. Alexander AE, Caldemeyer KS, Rigby P (1998) Clinical and surgical application of reformatted high-resolution CT of the temporal bone. Neuroimaging Clin N Am 8:31–50
2. Nayak S (2001) Segmental anatomy of the temporal bone. Semin Ultrasound CT MR 22:184–218
3. Casselman JW, Mermuys K, Delanote J et al (2008) MRI of the cranial nerves – more than meets the eye: technical considerations and advanced anatomy. Neuroimaging Clin N Am 18:197–231
4. Casselman JW, Safronova MM (2014) Imagerie des voies auditives et vestibulaires. In: Veillon F, Casselman JW, Meriot P et al (eds) Imagerie de l'oreille et de l'os temporal. Lavoisier, Paris, pp 227–238
5. Casselman JW, Delanote J, Kuhweide R et al (2015) Congenital malformations of the temporal bone. In: Lemmerling M, De Foer B (eds) Temporal bone imaging. Springer, Berlin/Heidelberg, pp 119–154
6. Veillon F, Riehm S, Emachescu B et al (2001) Imaging of the windows of the temporal bone. Semin Ultrasound CT MR 22:271–280
7. Veillon F, Baur P, Dasch JC et al (1991) Traumatismes de l'os temporal. In: Veillon F (ed) Imagerie de l'oreille. Médecine-Sciences Flammarion, Paris, pp 243–281
8. Casselman JW, Safronova MM (2014) IRM des traumatismes de l'os temporal et des régions adjacentes. In: Veillon F, Casselman JW, Meriot P et al (eds) Imagerie de l'oreille et de l'os temporal. Lavoisier, Paris, pp 747–760
9. Sartoretti-Schefer S (1997) Gadolinium-DTPA enhanced MRI of the facial nerve in patients with posttraumatic facial nerve palsy. AJNR Am J Neuroradiol 18:1115–1125
10. Swartz JD, Harnsberger HR (1998) The otic capsule and otodystrophies. In: Swartz JD, Harnsberger HR (eds) Imaging of the temporal bone. Thieme, New York, pp 240–317
11. Casselman JW, Mark AS, Butman JA (2009) Anatomy and diseases of the temporal bone. In: Atlas S (ed) Magnetic resonance imaging of the brain and spine, 4th edn. Lippincott Williams & Wilkins a Walters Kluwer Business, Philadelphia, pp 1193–1257
12. De Foer B, Vercruysse J-P, Pouillon M et al (2007) Value of high-resolution computed tomography and magnetic resonance imaging in the detection of residual cholesteatoma in primary bony obliterated mastoids. Am J Otolaryngol 28:230–234
13. De Foer B, Vercruysse J-P, Bernaerts A et al (2010) Value of non echo-planar diffusion-weighted MR imaging versus delayed post-gadolinium T1-weighted MR imaging for the detection of middle ear cholesteatoma. Radiology 255:866–872
14. De Foer B, Nicolay S, Vercruysse JP et al (2015) Imaging of cholesteatoma. In: Lemmerling M, De Foer B (eds) Temporal bone imaging. Springer, Berlin/Heidelberg, pp 69–88
15. Juliano AFT, Maya M, Lo WW et al (2011) Temporal bone tumors and cerebellopontine angle lesions. In: Som PM, Bergeron RT (eds) Head and neck imaging, 5th edn. Mosby Inc-affiliate of Elsevier Inc, St-Louis, pp 1449–1531
16. Casselman JW, Lu CH, De Foer B et al (2014) Schwannomes du nerf vestibulocochléaire. In: Veillon F, Casselman JW, Meriot P (eds) Imagerie de l'oreille et de l'os temporal. Lavoisier, Paris, pp 921–958
17. Tieleman A, Casselman JW, Somers T et al (2008) Imaging of intralabyrinthine schwannomas: a retrospective study of 52 cases with emphasis on lesion growth. AJNR Am J Neuroradiol 29:898–905
18. Somers T, Casselman J, de Ceulaer G et al (2001) Prognostic value of MRI findings in hearing preservation surgery for vestibular schwannoma. Am J Otol 22:87–94
19. Dubrulle F, Ernst O, Vincent C et al (2000) Enhancement of the cochlear fossa in the MR evaluation of vestibular schwannoma: correlation with success at hearing preservation surgery. Radiology 215:458–462
20. Mark AS (1994) Contrast-enhanced magnetic resonance imaging of the temporal bone. Neuroimaging Clin N Am 4:561–578
21. Kenis C, De Foer B, Casselman JW (2015) Inner ear pathology. In: Lemmerling M, De Foer B (eds) Temporal bone imaging. Springer, Berlin/Heidelberg, pp 219–235
22. Casselman JW, Kuhweide R, Ampe W et al (1996) Inner ear malformations in patients with sensorineural hearing loss: detection with gradient-echo (3DFT-CISS) MR imaging. Neuroradiology 38:278–286
23. Casselman JW, Offeciers FE, Govaerts PJ et al (1997) Aplasia and hypoplasia of the vestibulocochlear nerve: diagnosis with MR imaging. Radiology 202:773–781
24. Barath K, Schuknecht B, Monge Naldi B et al (2014) Detection and grading of endolymphatic hydrops in Menière disease using MR imaging. AJNR Am J Neuroradiol 35:1387–1392
25. Deplanque D, Godefroy O, Guerouaou D et al (1998) Sudden bilateral deafness: lateral inferior pontine infarction. J Neurol Neurosurg Psychiatry 64:817–818
26. Sasaki O, Ootsuka K, Taguchi K et al (1994) Multiple sclerosis presented acute hearing loss and vertigo. ORL J Otorhinolaryngol Relat Spec 56:55–59
27. Moonis G, Lo WWM, Maya M (2011) Vascular tinnitus of the temporal bone. In: Som PM, Curtin HD (eds) Head and neck imaging, 5th edn. Mosby Inc – affiliate of Elsevier Inc, St.-Louis, pp 1409–1422
28. Swartz JD, Harnsberger HR (1998) Temporal bone vascular anatomy, anomalies, and diseases, emphasizing the clinical-radiological problem of pulsatile tinnitus. In: Swartz JD, Harnsberger HR (eds) Imaging of the temporal bone. Thieme, New-York, pp 170–239
29. Casselman JW (2014) Imagerie des acouphènes. In: Veillon F, Casselman JW, Meriot P et al (eds) Imagerie de l'oreille et de l'os temporal. Lavoisier, Paris, pp 1523–1564